

Chapter 14

Precision Dressing and Truing of Diamond Grinding Wheel with V-tip



YanJun Lu, Jiangxiu Ouyang, and Yuming Huang

Abstract Due to low efficiency and environmental pollution in the traditional mechanical or EDM truing of the metal-bonded wheel, a novel method termed dry ECD (electro-contact discharge) truing was proposed to truing of V-tip diamond wheel with grain sizes of #600 and #1200 in this chapter. The effects of discharge parameters, such as pulse frequency, duty cycle, and open-circuit voltage, on the shape accuracy of the V-tip diamond wheel were investigated. The relationship between the V-tip angle/radius and discharge parameters was analyzed. The parameters were then optimized to obtain a high shape accuracy. On the other hand, to evaluate the grinding performances of the V-tip wheel after truing, a micro-grinding test was also conducted on cemented carbide to grinding grooves. The depth error, arc error and surface roughness of the ground groove were measured to evaluate the grinding performances of the V-tip wheel trued with the optimal parameters. The results revealed that the highest shape accuracy was obtained at pulse frequency of 4000 Hz, duty cycle of 50%, and open-circuit voltage of 25 V. As a result, the V-tip wheel obtained the minimum tip angle of 62.4° and the minimum tip radius of $15\ \mu\text{m}$. Simultaneously, the groove had the minimum depth error of $2.6\ \mu\text{m}$ and the minimum arc radius of $3.2\ \mu\text{m}$ on the surface of cemented carbide ground with the trued V-tip wheel. The surface roughness was $0.31\ \mu\text{m}$ on the surface of the ground groove.

Y. Lu (✉) · J. Ouyang · Y. Huang
Shenzhen Key Laboratory of High Performance Nontraditional Manufacturing, College of
Mechatronics and Control Engineering, Shenzhen University, Nan-Hai Ave 3688,
Shenzhen 518060, Guangdong, PR China
e-mail: luyanjun@szu.edu.cn

1 Introduction

The regular micro array structure at micron scale can now be fabricated on the surface of hard-brittle materials to achieve new levels of functionality [1]. However, surface machining of micro structures in difficult-to-machine materials is challenging. Precision grinding with diamond grinding wheel is known to be the most valid micro fabrication technique [2]. However, the dressing and truing of diamond grinding wheel is very significant. The efficiency and accuracy of truing are technical obstacles in industrialization.

It is very difficult to process the V-groove structure on the surfaces of hard and brittle materials because of its high melting point and fragility, so at present, in addition to precision grinding, there are other precision machining methods such as laser machining, ion beam, chemical etching and so on. For example, Zheng et al. used the high-energy laser to process micro-grooves on cemented carbide tools to explore their tribological properties [3]. Liu et al. used femtosecond laser equipment to process grooves at 45° to the main cutting edge on the carbide tool surface, latter cut Al_2O_3 -based ceramics by using it [4]. Lian proposed inductively coupled plasma etching cemented carbide to process micro-grooves and other micro-structures [5]. However, the energy consumption of laser processing and ion beam processing is several times that of grinding processing, which is complicated and the equipment expensive as well, the latter will also cause pollution problems of chemical waste liquid and other problems, while the precision grinding technology with V-shaped tip grinding wheel can ensure the shape precision and the surface quality of grooves simultaneously. The shape accuracy of the grooves after machining depends largely on the shape accuracy of the V-tip grinding wheel when grinding hard alloy grooves with v-tip grinding wheel, therefore, the grinding wheel needs to be carefully trued for several times before machining in order to better ensure the shape accuracy of the V-shaped grooves on the workpiece surface after machining.

Presently, methods of grinding wheel truing are mainly divided into three categories. The first category is traditional mechanical truing method, the second type is special truing method represented by discharge truing, electrolytic truing and laser pulse truing, and the third kind is the complementary truing method of traditional mechanical truing method and special truing method [6]. The traditional mechanical truing method is the most developed and mature truing method of them. Zhou et al. [7] realized the truing of arc diamond grinding wheel through three-axis coupling control, and pointing out it were significantly reduced that the arc error, radial runout error and radius fluctuation of the diamond grinding wheel after truing, especially the shape error of the processed aspheric lens was less than $4\ \mu\text{m}$. The traditional mechanical truing method has its advantages of simple process, mature technology and stable truing accuracy, but it as well has such defects as easy wear of truing tool, low truing efficiency, difficult tool measurement and compensation [8], moreover cause mechanical damage to diamond particles of grinding wheel. In order to solve the truing problem of metal bonded grinding wheels, Suzuki K applied electric discharge machining (EDM) [9] to the grinding field for the first time and proposed the

concept of electric discharge dressing (EDD) [10]. In principle, the discharge truing method is to take the machining tool as the negative pole while the workpiece as the positive pole, and make use of momentary and localized high temperature produced by the discharge between the two electrodes, which causes the fusion or evaporation of the metal bond of the grinding wheel, thus forming overlapping discharge pits on the surface of the grinding wheel to achieve the function of binding agent removal. As EDD avoids the vibration phenomenon that the traditional mechanical contact truing process, which greatly improves the truing accuracy and the integrity of grinding wheel grains [11]. Electrolytic in-process (ELID) truing [12] can effectively solve the sharpening problem of metal bond grinding wheel. According to its principle, adding an electrolyte between the electrode and the trued grinding wheel to make it dissolve under the action of electric current, at the same time, it produces a layer of oxide film on the surface of the grinding wheel to avoid its transition reaction. In the truing process, ELID can produce the truing amount that it is suitable for the wear of the grinding wheel in time to maintain a good grinding performance of it [13, 14]. Wu et al. [15] used ELID to make the dull abrasive particles fall off so timely that the grinding wheel always keeps its sharpness. Both ELID and EDD can be a solution to deal with the problem of metal bonded grinding wheel truing, but they requires the processing object is conductive material when using these two truing methods, and they cannot achieve the precision truing of the coarse-grained super-abrasive grinding wheels, need to be equipped with special power, the maintenance equipment is expensive as well [16]. In addition, the dielectric fluids and electrolytes will cause the problems of environmental contamination and equipment corrosion [17, 18]. For the shortcomings of traditional mechanical truing method and electrolytic truing method, Wang [19] proposed a new truing method, namely dry non-contact discharge assisted truing method, which can achieve high truing efficiency and good truing quality, but it has the disadvantages of poor multi-controllability and high processing cost due to the need to adjust discharge gap for many times in non-contact mode.

In view of various problems existed in the grinding wheel truing method mentioned above, an environmentally friendly and pollution-free dry electrical contact discharge (ECD) truing method [20, 21] is adopted in this chapter. Therefore, the ECD truing process was developed to achieve high efficiency and accuracy in grinding diamond V-tip. There is no need to take cutting fluid or waste liquid discharge and require expensive discharge gap control equipment because of the contact characteristics of it. Dry ECD truing not only allows the fine diamond abrasive grains to protrude without damaging the metal bond of the wheel, but also removes the bond tail behind the protruding abrasive grains. By adjusting discharge parameters, the angle and radius of V-shaped tip under different pulse discharge parameters were analyzed to achieve the highest shape accuracy. In order to test the effectiveness of V-shaped tip truing, micro-grinding experiments were carried out with cemented carbide materials, meanwhile, the grinding performance of trued diamond wheel was verified by observing the ground surface topography.

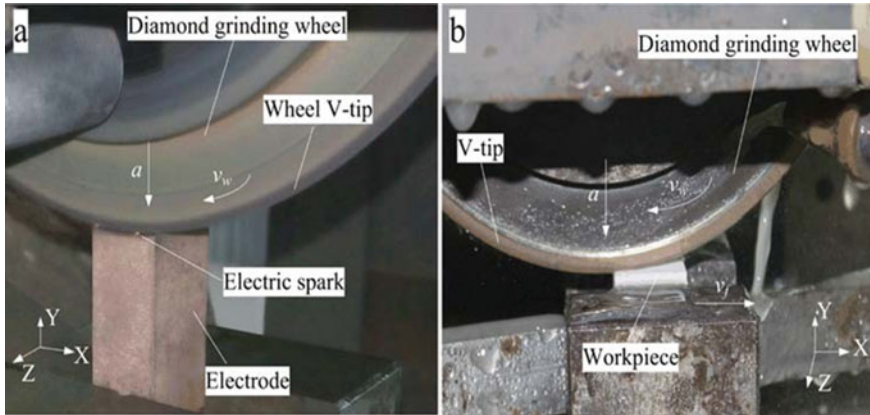


Fig. 1 Dry electro-contact discharge (ECD) truing and micro-grinding of V-tip diamond grinding wheel: **a** image of V-tip truing and **b** micro-grinding photo of trued V-tip diamond wheel

2 V-tip Truing of #600 Diamond Grinding Wheel Using Dry ECD

2.1 Experimental Setup of Dry ECD for #600 Diamond Grinding Wheel

The V-tip diamond wheel was used for grinding micro microcrystallite glass ceramics and SiC reinforced Al (Al/SiCp) composites. Micro-grinding machining technology were applied to create the micro-groove array structures and micro-pyramid array structures on the surfaces of these three materials. Figure 1b shows a picture of the micro-grinding with SD600 V-tip diamond wheel. The depth and space of the processed V-groove was $500\ \mu\text{m}$ and $570\ \mu\text{m}$, respectively. The detailed micro-grinding machining conditions of the SD600 diamond inserts were shown in Tables 1 and 2.

2.2 Results and Discussions

As shown in Fig. 2, the state of the protruding part of the micro grain. on the V-side surface of the diamond wheel were in very good condition. However, the micro tip of grinding wheel was dull. This is due to the excessive truing time of the ECD diamond wheels. There were a great number of protrusive diamond grains on the surface of the metal bond. As a result, V-shape tip on diamond grinding wheel can be produced during when ECD truing. A sharp micro-grain cutting edge was created on the surface

Table 1 The ECD truing conditions of SD600 diamond grinding wheel V-tip

CNC grinder	SMART B818
Diamond grinding wheel	SD600, metal bond, diameter $D = 160$ mm, width $B = 2$ mm
Tool truing path	Crossed V-shape interpolation path
Truing electrode	Hybrid electrode of Cu and SiC (#600); Size: $20 \times 50 \times 15$ mm
Discharge parameters	Pulse power supply, open-circuit voltage $E = 10 \sim 25$ V, pulse frequency $f = 1000 \sim 5000$ Hz, duty cycle $dc = 10 \sim 50\%$
Truing parameters	Wheel speed $v_w = 12.6 \sim 20.9$ m/s, feed speed $vf = 200 \sim 500$ mm/min, depth of cut $a = 1 \sim 10$ μm , cumulative feed depth $a = 0.05 \sim 0.1$ mm
Coolant	No

Table 2 Micro-grinding machining conditions of SD600 diamond grinding wheel

CNC grinder	SMART B818
Diamond grinding wheel	SD600, metal bond, diameter $D = 160$ mm, width $B = 2$ mm, wheel speed $v_w = 25.1$ m/s
Tool path	Horizontal reciprocating and crossed interpolation path
Rough machining	Feed speed $v_f = 600$ mm/min, depth of cut $a = 10$ μm , cumulative feed depth $a = 490$ μm
Finish machining	Feed speed $v_f = 300$ mm/min, depth of cut $a = 2$ μm , cumulative feed depth $a = 10$ μm
Workpieces	Microcrystallite glass ceramics (30×15 mm); SiC reinforced Al (Al/SiCp) composites (10×10 mm)
Coolant	Water

of the grinding wheel in the V-cut direction. Diamond grinding wheels with a trued V-tip can be used for micro-grinding of machining hard and brittle materials.

Figure 3 shows the effect of different pulse field parameters on V-tip angle φ of SD600 diamond grinding wheel. The matching V-tip angle φ were 88.9° and 89.4° for open-circuit voltages E of 5 V and 25 V, respectively. Compared to the setting theoretical angle of 90° , the errors of angles V-tip were only 1.1° and 0.6° (see Fig. 3a). As the pulse frequency f increases. the maximum angle φ of V first gradually decreases and then increases (see Fig. 3b), this is caused by arc discharge while excessive truing on the V-tip on the surface of the diamond grinding wheel. At pulse frequencies f of 4000–5000 Hz and duty cycle dc of 50%, the V-tip angle error realized a minimum value of 0.6° (see Fig. 3c).

Figure 4 shows the effect of different pulse discharge parameters on V-tip radius r_v of SD600 diamond grinding wheel. The V-tip radius r_v increases as the open-circuit voltage E increases (see Fig. 4a). When the open-circuit voltage E was 5 V, the trued V-tip radius of diamond wheel reached a minimum value of 33 μm . The V-tip radius r_v was 44 μm and 78 μm respectively when the pulse frequency f is 4000 Hz and 5000 Hz (see Fig. 4b). Due to the inhomogenous electrical spark discharge caused

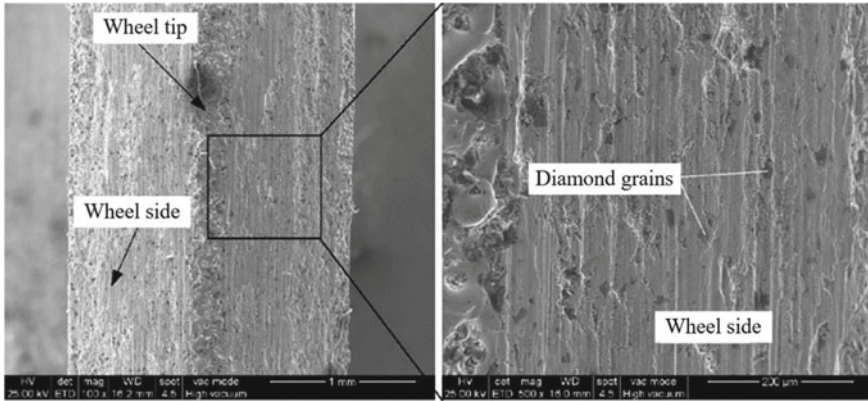


Fig. 2 V-shape tip and its protrusion topographies of SD600 diamond wheel after dry ECD truing

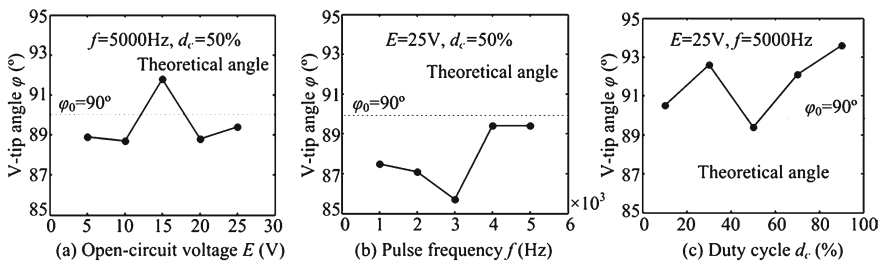


Fig. 3 The V-tip angles ϕ of SD600 diamond grinding wheel versus different pulse discharge parameters: **a** open-circuit voltage E , **b** pulse frequency f and **c** duty cycle dc

by large and little duty cycle, the V-tip radius r_v first decreased gradually and then boosted with the increase of duty cycle dc (see Fig. 4c). The peak radius V reaches a minimum value of $78 \mu\text{m}$ when the duty cycle dc was 50%. As a result, at the optimal parameters of the pulse discharge ($E = 5 \text{ V}$, $f = 4000 \text{ Hz}$, $dc = 50\%$), the minimum errors of V-tip angle and radius of SD600 diamond grinding wheel after ECD truing was 1.1° and $33 \mu\text{m}$, respectively.

Figure 5 shows the ground surface topography of microcrystallite glass ceramics after micro-grinding with the trued SD600 V-diamond grinding wheel. It can be concluded that after grinding, the surface of micro-groove and micro-pyramid structured surfaces were very smooth as well as the edges are undamaged. In addition, the V-tip shape at the ends of the micro-grooves and micro-pyramids spire was also very intact. However, the surface of microcrystallite glass ceramics contained many microscopic holes. This is due to the high fragility of microcrystalline glass ceramics.

Figure 6 shows the ground surface topography of SiC-reinforced Al composites (Al/SiCp) after micro-grinding with an SD600 V-tip diamond grinding wheel. In contrast to the surface of microcrystalline glass and reaction sintered SiC ceramics,

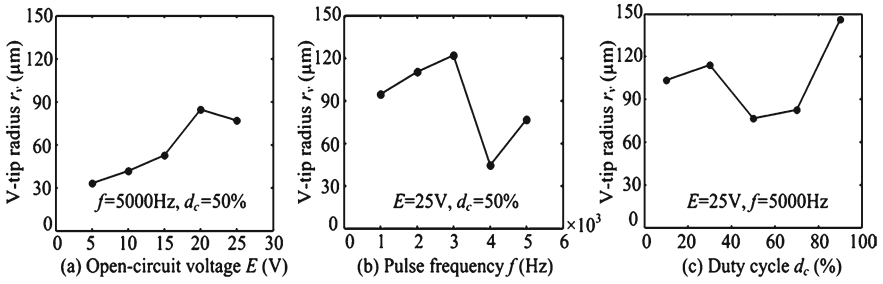


Fig. 4 Shows the V-tip radius r_v of SD600 diamond grinding wheel versus different pulse discharge parameters: **a** open-circuit voltage E , **b** pulse frequency f and **c** duty cycle d_c

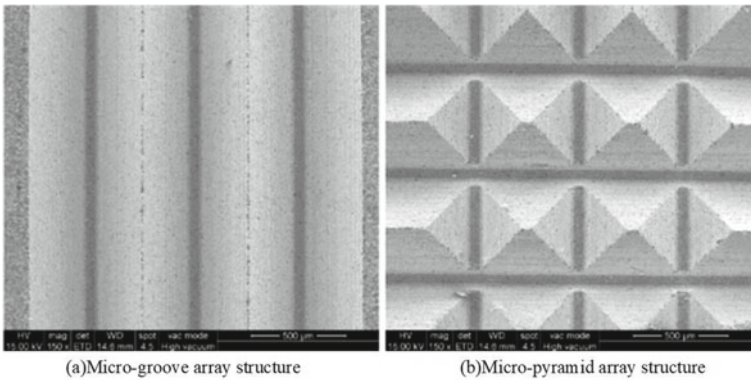


Fig. 5 The ground surface topography of microcrystallite glass ceramics after micro-grinding: **a** micro-groove array structure and **b** micro-pyramid array structure

the SiC-reinforced Al composites had the worst surface machining quality. In addition, the crack of micro-groove tip was very severe, with several burrs at the edge of micro-pyramid. This is due to the fact that the aluminum substrate contained SiC particles. In the grinding process of Al/SiCp composites, collision or brittle rupture occurred very easily. This made the processing of Al/SiCp composites very difficult.

3 V-tip Truing of #1200 Diamond Grinding Wheel Using Dry ECD

3.1 Experimental Setup

The experiments were performed on a CNC grinder (SMART-B818) in air, as shown in Fig. 7. The V-tip truing schematic diagram and setup of diamond grinding wheel

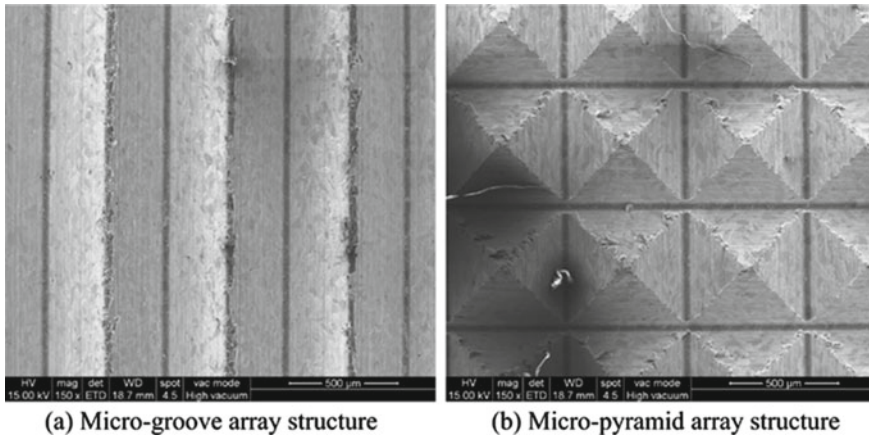


Fig. 6 The ground surface topography of SiC reinforced Al composites after micro-grinding: **a** micro-groove array structure and **b** micro-pyramid array structure

based on dry electro-contact discharge (ECD), the pulse power supply was linked between hybrid electrode (Cu and SiC) and metal-bonded diamond grinding wheel through conductive graphite brush (see Fig. 7a), and the cut machining along with electrical spark discharge was produced when the rotating grinding wheel was driven to grind electrode along a defined V-shape truing path, gradually, the V-shape tip of diamond grinding wheel was produced (see Fig. 7b). After truing and forming the V-shape tip of diamond grinding wheel, the precision truing experiments of SD1200 diamond grinding wheel using dry ECD were conducted by changing the pulse discharge parameters, including open-circuit voltage E , pulse frequency f and duty cycle dc derived from pulse power supply. Certain discharge energy levels were considered by adjusting the pulsed discharge parameters to explore their effect on material removal modes, as described in Table 3. They were shown in Table 1 that the detail dry ECD truing conditions of SD1200 diamond grinding wheel V-tip. Table 3

3.2 Experimental of Dry Micro-grinding

Using trued diamond grinding wheel for experimental of dry micro-grinding on the surfaces of cemented carbide, as Fig. 8 shows dry micro-grinding machining schemes and photo of cemented carbide using trued V-tip diamond grinding wheel. The trued diamond grinding wheel with V-tip was employed to process micro-groove and micro-pyramid array structures on the surfaces of cemented carbide using micro-grinding machining technology (see Fig. 8a, b). The dry micro-grinding photo of cemented carbide without any coolant using trued SD1200 V-tip diamond wheel was shown in Fig. 8c, which uses 200 μm as the ground V-groove depth of trued

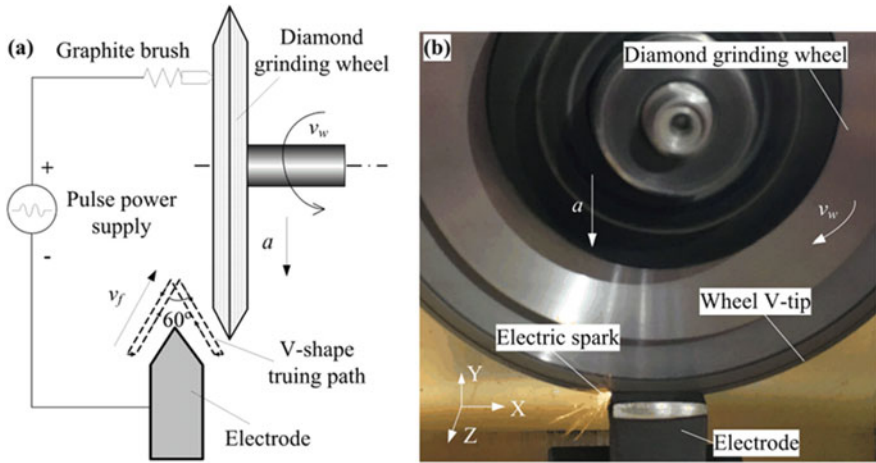


Fig. 7 Dry electro-contact discharge (ECD) truing of diamond grinding wheel V-tip: **a** V-tip truing scheme of diamond wheel and **b** V-tip truing image

Table 3 The ECD truing conditions of SD1200 diamond grinding wheel V-tip

CNC grinder	SMART B818	
Diamond grinding wheel	SD1200, metal bond, diameter $D = 150$ mm, width $B = 2.5$ mm	
Tool truing path	Crossed V-shape interpolation path	
Truing electrode	Hybrid electrode of Cu and SiC (#1200); Size: $L \times B \times H = 20 \times 50 \times 15$ mm	
Discharge parameters	Pulse power supply, open-circuit voltage $E = 5 \sim 25$ V, pulse frequency $f = 1000 \sim 5000$ Hz, duty cycle $d_c = 10 \sim 80\%$	
Truing parameters	Wheel speed $v_w = 18.8$ m/s, feed speed $v_f = 200$ mm/min, depth of cut $a = 1 \mu\text{m}$	
Coolant	No	
Pulse discharge parameters	1	$E = 25$ V, $f = 5000$ Hz, $d_c = 50\%$
	2	$E = 15$ V, $f = 5000$ Hz, $d_c = 50\%$
	3	$E = 5$ V, $f = 5000$ Hz, $d_c = 50\%$
	4	$E = 25$ V, $f = 4000$ Hz, $d_c = 50\%$
	5	$E = 25$ V, $f = 1000$ Hz, $d_c = 50\%$
	6	$E = 25$ V, $f = 5000$ Hz, $d_c = 10\%$
	7	$E = 25$ V, $f = 5000$ Hz, $d_c = 80\%$

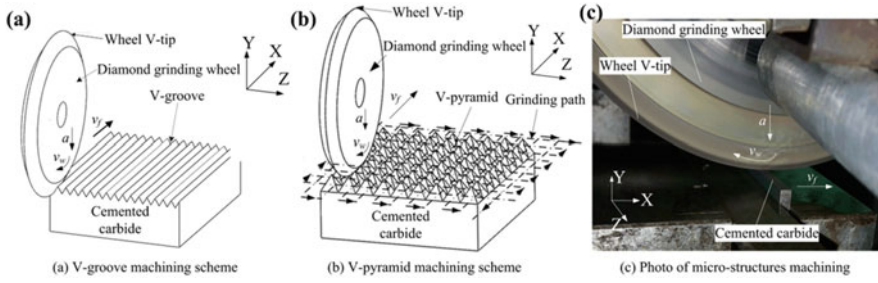


Fig. 8 Dry micro-grinding machining schemes and photo of cemented carbide: **a** V-groove machining scheme, **b** V-pyramid machining scheme and **c** micro-grinding image

Table 4 Dry micro-grinding conditions of cemented carbide using trued V-tip diamond grinding wheel

CNC grinder	SMART B818
Diamond grinding wheel	SD1200, metal bond, diameter $D = 150$ mm, width $B = 2.5$ mm; Wheel speed $v_w = 18.8$ m/s
Workpiece	Cemented carbide
Rough grinding	depth of cut $a = 5$ μm , cumulative feed depth $\Sigma a = 190$ μm ; feed speed $v_f = 50$ mm/min
Finish grinding	depth of cut $a = 1$, cumulative feed depth $\Sigma a = 10$ μm ; feed speed $v_f = 10$ mm/min
Coolant	No

V-tip diamond wheel. The detail micro-grinding machining conditions of SD1200 diamond grinding wheel were shown in, Tables 3 and 4.

3.3 Measurements

To obtain the V-tip profiles of trued diamond grinding wheel, the surface profiler (TALYSURF CLI 1000) and white light interferometer (WLI, BMT SMS Expert 3D) were used to measure the V-groove profiles by replicating the V-tip profile on the surface of the graphite plate, in the meanwhile, the surface topographies of trued diamond grinding wheel and ground cemented carbide workpieces were presented by scanning electron microscope (SEM, FEI Quanta 200) and 3D laser scanning microscope (VK-250, Keyence).

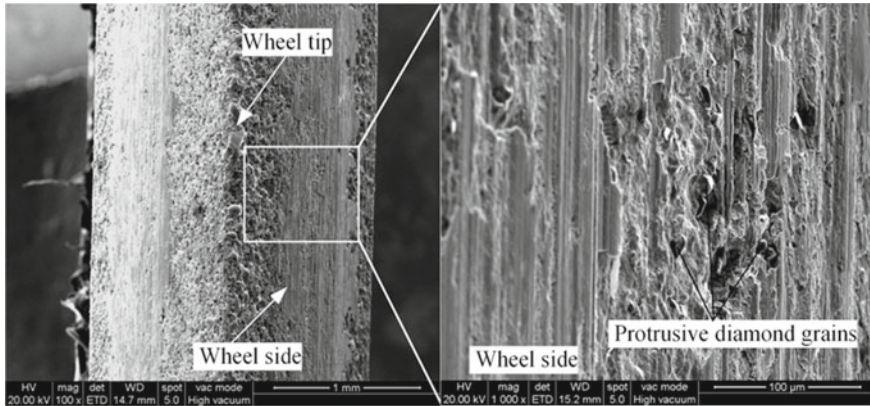


Fig. 9 SEM images of rough trued SD1200 V-tip diamond grinding wheel

3.4 Results and Discussions

3.4.1 Morphology of Rough Trued Tip Diamond Grinding Wheel

Figure 9 shows the SEM photos of rough trued SD1200 V-tip diamond grinding wheel after dry ECD. It is shown that the micro tip of diamond grinding wheel was roughly trued into the V-shape with a large V-tip radius, which is caused by the uneven roundness of the grinding wheel, the cutting edges of diamond grains on the side of grinding wheel were protruded out of the metal bond, however, the scratch on the side of grinding wheel was relatively serious. It may be because that the short circuit occurred when processing electrical discharge truing, resulting in the mutual scratch between the silicon carbide particles derived from hybrid electrode and metal bond on the surface of grinding wheel.

3.5 Morphology of Fine Trued Tip Diamond Grinding Wheel

As shown in Fig. 10, the SEM photos of fine trued SD1200 V-tip diamond grinding wheel after dry ECD is presented. In comparison with Fig. 9, as seen from Fig. 10, the V-shape tip of diamond grinding wheel become more sharp and the V-tip arc radius significantly decreased. Besides, due the micro-discharge can remove the metal binder around the abrasive particles, there is no binder tail, the wheel surface was relatively smooth and there were also many protrusive diamond micro-grains on the surface of the grinding wheel, which were beneficial for conducting precise micro-grinding machining.

As shown in Fig. 11, the section profiles of SD1200 diamond grinding wheel before and after truing forming is presented. As shown in Fig. 11a, the section contour

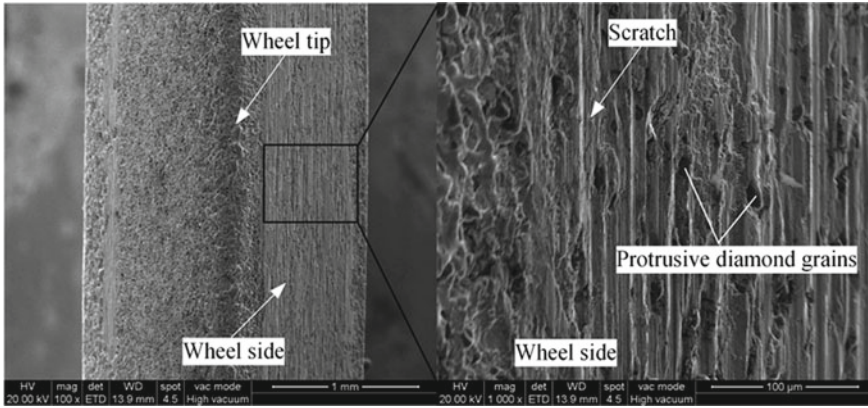


Fig. 10 SEM images of fine trued SD1200 V-tip diamond grinding wheel

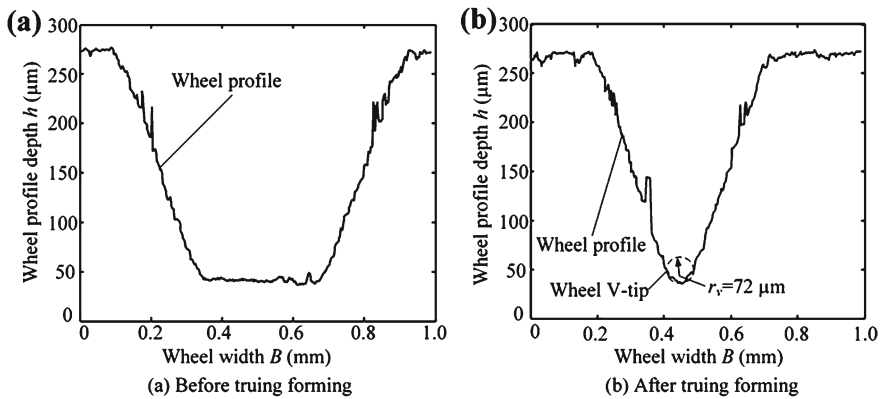


Fig. 11 The section profiles of SD1200 V-tip diamond grinding wheel before and after truing forming: **a** before truing forming and **b** after truing forming

of the diamond grinding wheel micro tip was trapezoidal before truing forming, while the V-shaped section contour of the diamond grinding wheel micro tip was presented after truing forming, and the V-tip radius r_v of the diamond grinding wheel was about 72 μm.

3.6 Influences of Impulse Discharge Parameters on V-tip Profiles of Diamond Grinding Wheel

Figure 12 shows the trued V tip profiles of SD1200 diamond grinding wheel under various pulse discharge parameters. It is shown that the V-tip contour shape

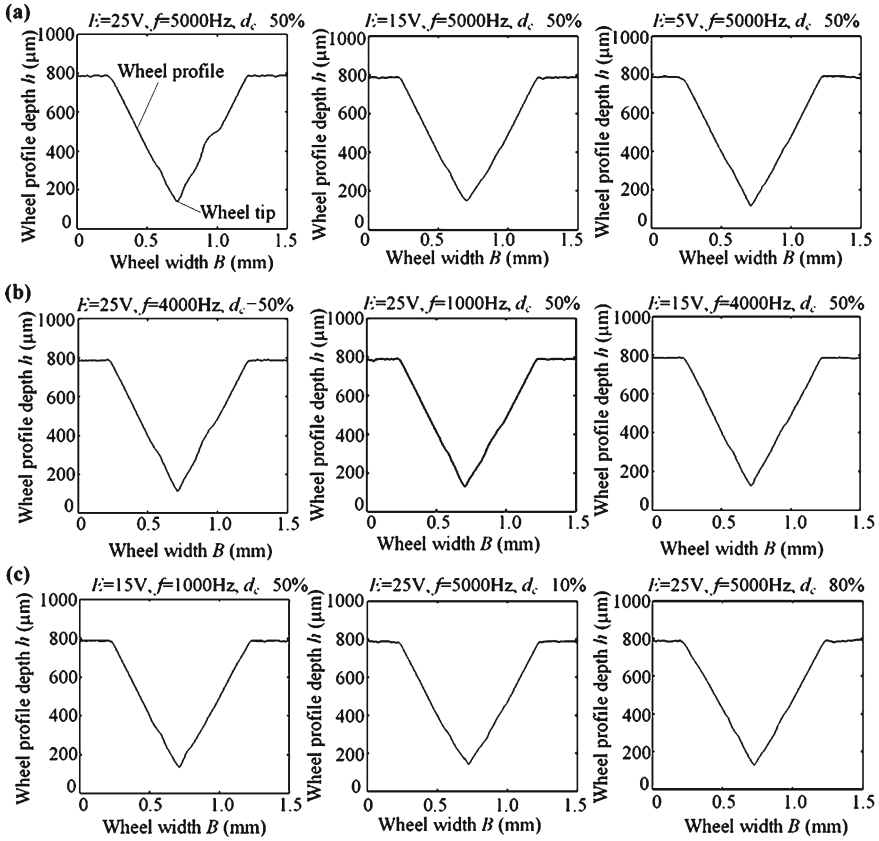


Fig. 12 The V-tip profiles of trued SD1200 diamond grinding wheel under different pulse discharge parameters: **a** open-circuit voltage E , **b** pulse frequency f and **c** duty cycle d_c

of diamond grinding wheel after truing under various pulse discharge parameters conditions was basically similar, nonetheless the V-tip angle and V-tip radius were different.

3.7 Influences of Impulse Discharge Parameters on V-tip Angle of Diamond Grinding Wheel

Figure 13 shows the influences of impulse discharge parameters on V-tip angle of SD1200 diamond grinding wheel. As shown in Fig. 13a, with the rise of open-circuit voltage E , the V tip angle φ first increased and then decreases, when the open-circuit voltage E was 25 V, the trued V tip angle reached a minimum value of 62.4° , and with the increase of pulse frequency f , the V tip angle φ first decreased and then increased

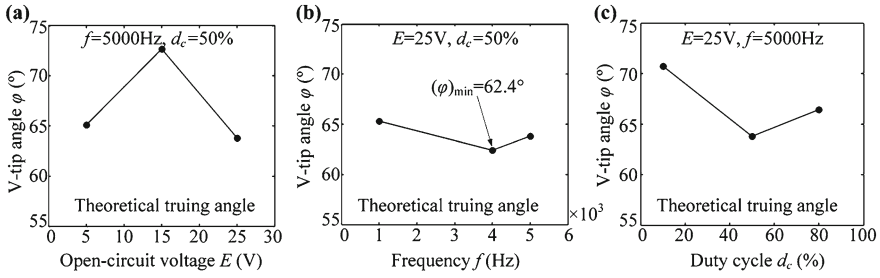


Fig. 13 The V-tip angles ϕ of trued SD1200 diamond grinding wheel under different pulse discharge parameters: **a** open-circuit voltage E , **b** pulse frequency f and **c** duty cycle d_c

(see Fig. 13b). This is because Low frequency leads to low energy, and the main truing process is machine grinding, the wheel with V-tip would be easily burned in high impulse discharge power and high pulse frequency. Either too high or too low discharge frequency increases the tip angle to some extent. In the other hand, when frequency f was 4000 Hz, the trued V tip angle also realized the minimum value of 62.4° , and with the increase of duty cycle d_c , the V tip angle ϕ first decreased and then increased (see Fig. 13c)., when duty cycle d_c was 50%, the trued V tip angle also reached the minimum value of 62.4° . This is because when the duty cycle is small or large, it will lead to uneven discharge. In contrast with the theoretical V-tip angle of 60° according to the setting truing path, the angle error of the trued V-tip was 2.4° .

3.8 Influences of Impulse Discharge Parameters on V-tip Radius of Diamond Grinding Wheel

As shown in Fig. 14, the influences of pulse discharge parameters on the V-tip radius r_v of trued SD1200 diamond grinding wheel is presented. With the increase of open-circuit voltage E , the V-tip radius r_v first increased and then decreased (see Fig. 14a). As the open-circuit voltage E were 5 V and 25 V, the trued V-tip radius r_v were $28\ \mu\text{m}$ and $29\ \mu\text{m}$, respectively. With the increase of pulse frequency f , V-tip radius r_v first decreased and then increased (see Fig. 14b).

When pulse frequency f was 4000 Hz, the trued V-tip radius r_v realized a minimum value of $15\ \mu\text{m}$. The V-tip radius r_v decreased with the increase of duty cycle d_c (see Fig. 14c), this is because the larger duty cycle was, the longer pulse discharge duration time and micro spark discharge time were and more fully dressed the grinding wheel is. When duty cycle d_c was 80%, the trued V-tip radius r_v reached a minimum value of $21\ \mu\text{m}$. However, too large duty cycle will cause the angle of V-tip to become larger. Therefore, in the V-tip truing process of SD1200 diamond grinding wheel, the better pulse discharge parameters including open-circuit voltage E , pulse frequency f and duty cycle d_c were 25 V, 4000 Hz and 50%, respectively, under the optimal pulse discharge parameters, namely, the open-circuit voltage E of 25 V, pulse frequency f

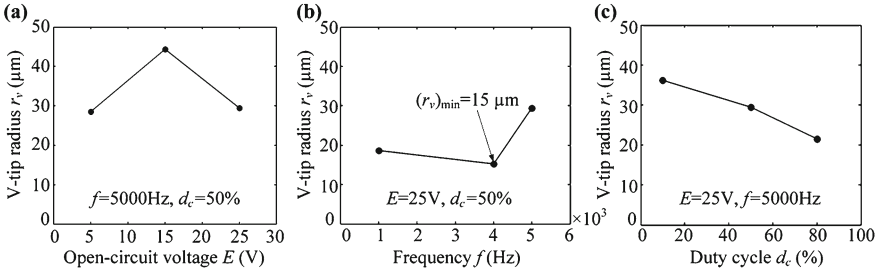


Fig. 14 The V-tip radius r_v of trued SD1200 diamond grinding wheel under different pulse discharge parameters: **a** open-circuit voltage E , **b** pulse frequency f and **c** duty cycle d_c

of 4000 Hz and duty cycle d_c of 50%, the minimum V-tip radius of trued SD1200 diamond grinding wheel was 15 μm .

3.9 Micro-topography and Form-Accuracy of Ground Micro-structured Cemented Carbide Surface

Figure 15 shows the V-groove morphologies of micro-ground cemented carbide before and after the V-tip truing forming of SD1200 diamond grinding wheel. The section contour of diamond grinding wheel was trapezoidal before V-tip truing forming, therefore, the section contour of micro-ground V-groove was also trapezoidal and the trued angle was 121° (see Fig. 15a), and in contrast with the theoretical truing angle of 120° , the angle error was only 1° . After the V-tip truing forming, the section contour of diamond grinding wheel was V-shaped so that the section contour of micro-ground V-groove was also V-shaped. The measured V-tip angle φ and V-tip radius r_v was 64.2° and $78 \mu\text{m}$, respectively, then compared with the theoretical V-groove angle of 60° , the micro-ground V-tip angle error was 4.2° . Since the V-tip arc radius of grinding wheel section contour before machining cemented carbide was $72 \mu\text{m}$, it indicates that the V-tip of grinding wheel was worn.

Figure 16 shows the surface morphologies of micro-ground cemented carbide. As shown in Fig. 16, the tip and bottom of V-groove can be clearly seen. The bottom of V-groove had a tiny arc, which indicates that the grinding wheel tip was worn in the grinding process of cemented carbide.

Figure 17 shows the V-groove profile on the cemented carbide surface. From the figure, it can be observed that the minimum error between the groove depth and the theoretical depth of $200 \mu\text{m}$ is only $2.6 \mu\text{m}$, and the maximum depth error is $11.7 \mu\text{m}$. Compared with the grinding wheel tip radius of $15 \mu\text{m}$, the minimum error of the bottom arc radius is $3.2 \mu\text{m}$, and the maximum error is $7.3 \mu\text{m}$. As the grinding progresses, the error of the bottom arc radius of the groove gradually increases, which indicates that the grinding wheel tip is worn and the V groove is worn. The difference between the groove angle and the theoretical angle of 60° is

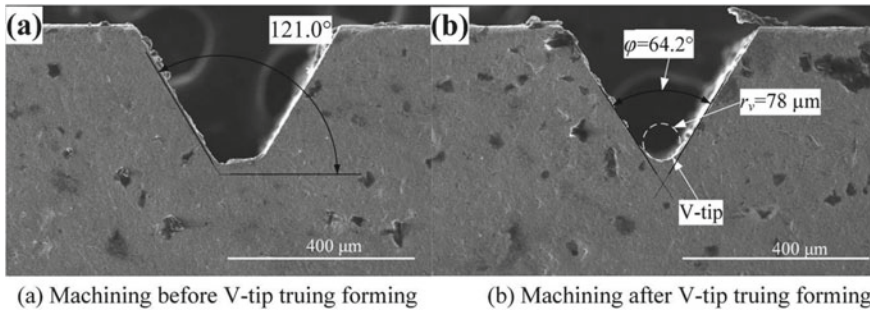


Fig. 15 SEM photos of micro-ground V-groove on the surfaces of cemented carbide before and after V-tip truing forming: **a** before V-tip truing forming and **b** after V-tip truing forming

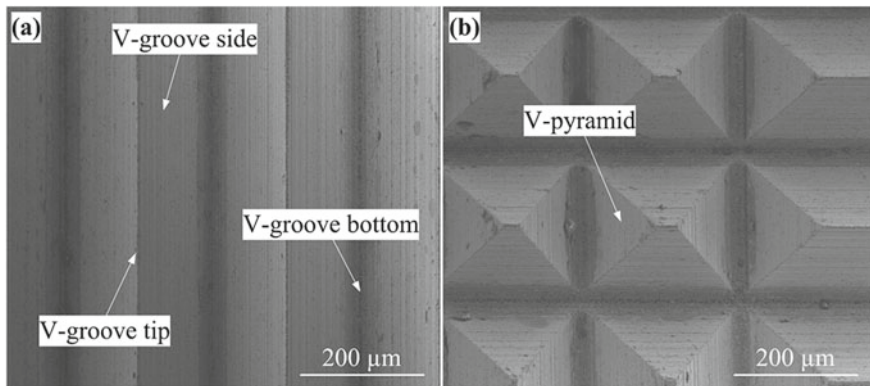


Fig. 16 SEM photos of micro-ground micro-structured cemented carbide surface: **a** V-grooved array structures surface and **b** V-pyramid array structures surface

very small, indicating that grinding in the plastic domain of the micro-structure of the cemented carbide surface can ensure a better shape error.

4 Conclusions

The ECD dry truing method can achieve the V-tip truing of diamond with high efficient and precise. The pulse field parameters were optimized in repeated V-tip truing test. The optimal parameters for pulse trimming were open-circuit voltage of 5 V, pulse frequency of 4000 Hz and duty cycle of 50%. After ECD cutting, sharp micro grain cutting edges were formed on the surface of the wheel. The minimum V-tip angle error and radius of trued SD600 V-tip diamond grinding wheel reached 1.1° and $33\ \mu\text{m}$, respectively. The trued V-tip diamond wheel can be used to fabricate regular and smooth micro-groove and micro-pyramid array structures on the surfaces

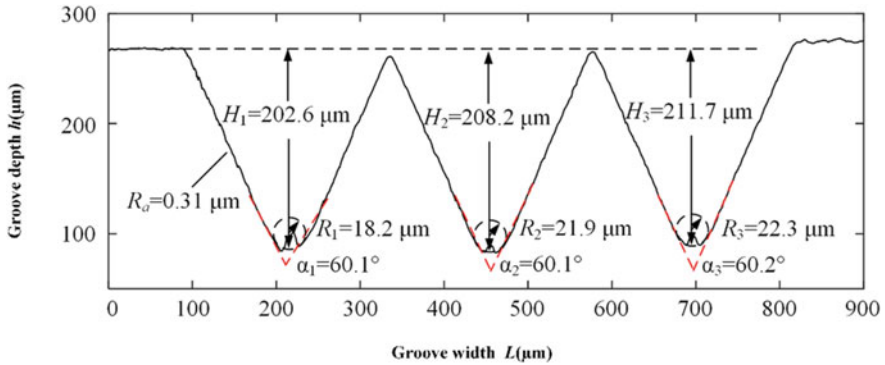


Fig. 17 Cemented carbide surface V-groove profile curve

of hard and brittle materials such as microcrystalline glass ceramics and Al/SiCp composites.

The truing technology of grinding wheel V-tip with dry contact discharge (ECD) is put forward in this chapter, the influence of pulse discharge parameters on the truing effect of metal base grinding wheel tip is studied to achieve efficient and precise truing of grinding wheel, whose conclusion is of guiding significance to the truing process optimization of diamond grinding wheel used in cemented carbide microstructure manufacturing. The specific conclusions are shown as follows:

- (1) The ECD truing technology, which can settle several issues concerning low truing efficiency of metal fund diamond grinding wheel, uncertainty of accuracy and special structure truing requirements, to obtain diamond grinding wheel with good cutting edge effect and high shape accuracy.
- (2) The precise truing of V tip of #1200 diamond grinding wheel can be achieved by applying ECD technology, whose optimal truing pulse discharge parameters are $E = 25$ V, $f = 4000$ Hz, $d_c = 50\%$. Under those parameters it can realize the minimum radius of arc of grinding wheel tip after truing and the minimum angle error of grinding wheel tip, which are $15 \mu\text{m}$ and 2.4° respectively.
- (3) It is beneficial to realize plastic domain machining of hard alloy surface microstructure, obtain surface microstructure with high shape precision and low error and high surface quality by adapting diamond grinding wheel with good cutting edge effect. The minimum error of groove depth and the minimum error of bottom arc radius are respectively $2.6 \mu\text{m}$, $3.2 \mu\text{m}$, additionally the average roughness of groove side is $0.31 \mu\text{m}$ as the results show.

Acknowledgements The work described in this chapter was supported by the National Natural Science Foundation of China (Grant No. 51805334), the China Postdoctoral Science Foundation [Grant No. 2016M602460], the Science and Technology Planning Project of Guangdong Province [Grant Nos. 2016A040403043 and 2017A010102003] and the International Science and Technology Cooperation Project of Shenzhen City (Grant No. GJHZ20190822091805371).

References

1. Egashira K, Hosono S, Takemoto S, Masao Y (2011) Fabrication and cutting performance of cemented tungsten carbide micro-cutting tools. *Precis Eng* 35:547–553
2. Zhao QL, Guo B (2011) Ultraprecision grinding technology of microstructured optical functional molds. *J Mech Eng* 47:177–185
3. Zheng G, Lin Y (2021) Tribological properties of micro-groove cemented carbide by laser processing. *Micromachines* 12:486
4. Tan JH, Wong WLE, Dalgarno KW (2017) An overview of powder granulometry on feedstock and part performance in the selective laser melting process. *Addit Manuf* 18:228–255
5. Lian Y, Mu C, Xie C, Yao B (2019) Experimental investigation of inductively coupled plasma etching on cemented carbides. *Vacuum* 162:101–109
6. Deng H, Xu Z (2019) Dressing methods of superabrasive grinding wheels: a review. *J Manuf Process* 45:46–69
7. Zhou L, Wei Q, Zheng N et al (2019) Dressing technology of arc diamond wheel by roll abrading in aspheric parallel grinding. *Int J Adv Manufact Technol* 105:2699–2706
8. Chen B, Guo B, Zhao Q (2018) Online monitoring of truing arc-shaped diamond wheel by acoustic emission signal. *Proc Inst Mech Eng Part B J Eng Manufact* 232:1484–1490
9. Wang X, Ying B, Liu W (1996) EDM dressing of fine grain super abrasive grinding wheel. *J Mater Process Technol* 62:299–302
10. Yu J, He L, Huang S et al (2015) State-of-the-art of electrical discharge dressing technology for superabrasive grinding wheel. *China Mech Eng* 26:2254
11. Zhang FH, Kang GW, Yang YS et al (2006) EDM dressing for metal-bond super hard arc-forming wheel. In: *Key Engineering Materials*. Trans Tech Publ, pp 99–103
12. Kuai J, Zhang H (2019) Research on generation and polishing mechanisms of nano grain α -Fe₂O₃ in precision electrolytic in process dressing (ELID) grinding. *Proc Manufact* 37:425–430
13. Mao C, Zhou F, Hu Y et al (2019) Tribological behavior of cBN-WC-10Co composites for dry reciprocating sliding wear. *Ceram Int* 45:6447–6458
14. Mao C, Lu J, Zhao Z et al (2018) Simulation and experiment of cutting characteristics for single cBN-WC-10Co fiber. *Precis Eng* 52:170–182
15. Wu Q, Ouyang Z, Wang Y et al (2019) Precision grinding of engineering ceramic based on the electrolytic dressing of a multi-layer brazed diamond wheel. *Diam Relat Mater* 100:107552
16. Xxx DH, Xu Z (2019) Dressing methods of superabrasive grinding wheels: A review. *J Manuf Process* 45:46–69
17. Wu Q, Wang Y, Qu W, Deng Z (2017) Research status and perspectives of ELID grinding fluid. *China Mech Eng* 28:1118
18. Wegener K, Hoffmeister H-W, Karpuschewski B et al (2011) Conditioning and monitoring of grinding wheels. *CIRP Ann* 60:757–777
19. Wang Y, Zhou X, Hu D (2006) An experimental investigation of dry-electrical discharge assisted truing and dressing of metal bonded diamond wheel. *Int J Mach Tools Manuf* 46:333–342
20. Lu YJ, Li LJ, Xie J, et al (2017) Dry electrical discharge dressing and truing of diamond grinding wheel V-tip for micro-grinding. In: *2017 5th International conference on mechatronics, materials, chemistry and computer engineering (ICMMCCE 2017)*. Atlantis Press, pp 548–552
21. He Q, Xie J, Lu K, Yang H (2020) Study on in-air electro-contact discharge (ECD) truncating of coarse diamond grinding wheel for the dry smooth grinding of hardened steel. *J Mater Process Technol* 276:116402